

# Effect of alkali and alkaline earth metal ions on the catalytic epoxidation of styrene with molecular oxygen using cobalt(II)-exchanged zeolite X

Jince Sebastian, Krishna Mohan Jinka, Raksh Vir Jasra \*

*Silicates and Catalysis Discipline, Central Salt and Marine Chemicals Research Institute, G.B. Marg, Bhavnagar-364 002, Gujarat, India*

Received 8 June 2006; revised 24 August 2006; accepted 1 September 2006

Available online 11 October 2006

## Abstract

Liquid-phase catalytic epoxidation of styrene to styrene epoxide was carried out at 373 K using molecular oxygen at atmospheric pressure, in the presence of Co(II)-exchanged zeolite X. Styrene conversion of >99% with styrene oxide selectivity up to 68% was achieved using NaCoX. Alkali and alkaline earth metal cations were introduced into the zeolite catalyst to increase styrene conversion and styrene oxide selectivity. Replacing the sodium ions with alkali metal cations increased styrene oxide selectivity from 68% for NaCoX19 to 77% for CsCoX20. Styrene oxide selectivity further increased on replacing the sodium ions with alkaline earth metal cations, and styrene oxide selectivity up to 85% and styrene conversion >99% was obtained with CaCoX, SrCoX, and BaCoX. This is the first report of such a high styrene epoxide selectivity with a heterogeneous catalyst observed for styrene epoxidation using molecular oxygen. The presence of a small amount of water in the reaction system increases styrene conversion without affecting styrene oxide selectivity. The cobalt-exchanged zeolite X catalysts showed similar catalytic activity even after three catalytic reaction cycles.

© 2006 Elsevier Inc. All rights reserved.

**Keywords:** Molecular oxygen; Styrene; Styrene oxide; NaCo(II)X; Epoxidation; Alkali and alkaline earth-exchanged zeolite X

## 1. Introduction

Styrene oxide is a commercially important intermediate used in the synthesis of fine chemicals and pharmaceuticals. Conventionally, it is produced using one of two methods, namely dehydrochlorination of styrene chlorohydrin with a base or oxidation of styrene using organic peracids. Both these methods use hazardous chemicals and show poor selectivity for styrene epoxide, thus leading to the generation of undesirable products. Consequently, attempts have been made to replace the conventional route for the epoxidation of alkenes by environmentally friendly reusable heterogeneous catalysts such as Ti/SiO<sub>2</sub> [1–3], TS-1 [3–7], Ti-MCM-41 [6], Fe or V/SiO<sub>2</sub> [3], TBS-2, TS-2 [7],  $\gamma$ -Al<sub>2</sub>O<sub>3</sub> [8], and gold supported on Al<sub>2</sub>O<sub>3</sub>, Ga<sub>2</sub>O<sub>3</sub>, In<sub>2</sub>O<sub>3</sub>, Tl<sub>2</sub>O<sub>3</sub> [9] MgO, and other alkaline earth oxide [10] catalysts, using TBHP [1,9–11], H<sub>2</sub>O<sub>2</sub> [2–4,6–8], or urea–H<sub>2</sub>O<sub>2</sub> adduct [9] as an oxidizing agent. Although styrene conversion

is very high when H<sub>2</sub>O<sub>2</sub> is used as an oxidizing agent, the selectivity for styrene oxide is poor. On the other hand, using TBHP [1] and urea–H<sub>2</sub>O<sub>2</sub> adduct [5] as oxidizing agents yields high styrene oxide selectivity (>80%) with low styrene conversion (9.8 and 17.7%, respectively).

Molecular oxygen is the most desirable oxidant for the epoxidation of alkenes with respect to environmental and economic considerations. Cobalt ions and complexes are well-known catalysts for the selective oxidation of alkanes and alkylbenzenes with O<sub>2</sub> [12]. Cobalt complexes have also been used for the epoxidation of alkenes with *tert*-butyl hydroperoxide (TBHP) and iodosylbenzene [13]. The catalytic oxidation of terminal olefins, including styrene, by O<sub>2</sub> to the corresponding 2-ketones and 2-alcohols using a cobalt(II) complex has been reported [14,15]. Cobalt salen complexes were reported to show catalytic activity for epoxidation of styrene with O<sub>2</sub>, although a sacrificial co-reductant, isobutyraldehyde, was necessary [16]. CoCl<sub>2</sub> was investigated for the oxidation of monoterpenes with O<sub>2</sub>, and it was found that the allylic oxidation proceeded predominantly [17]. Ruthenium complexes, ruthenium- and iron-substituted polyoxometalates, have been reported [28,29] as

\* Corresponding author. Faxes: +91 278 2567562, +91 278 2566970.  
E-mail address: [rvjasra@csmcri.org](mailto:rvjasra@csmcri.org) (R.V. Jasra).

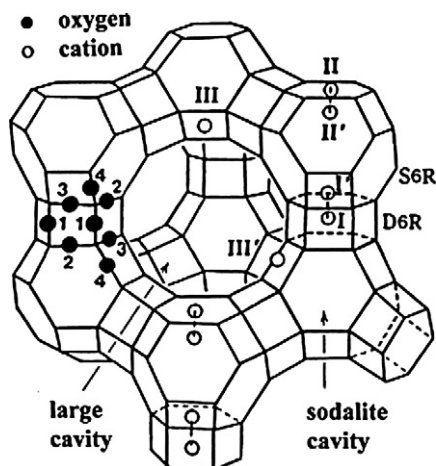


Fig. 1. The framework structure of zeolite X, near the centre of each line segment is an oxygen atom. The numbers 1–4 indicate the different oxygen atoms. Silicon and aluminium atoms alternate at the tetrahedral intersections, except that Si substitutes for Al at about 4% of the Al positions. Extra framework cation positions are labeled with Roman numerals.

homogeneous catalysts for the epoxidation of alkenes using molecular oxygen without the need for a co-reductant, but such reports with heterogeneous catalysts are sparse. Heterogeneous cobalt catalysts have been reported for the selective oxidation of alkanes, especially cyclohexane, and alkenes [18–27], but there are few studies using heterogeneous catalysts for epoxidation of alkenes with molecular oxygen without needing a co-reductant. Immobilized cobalt complexes in organo-modified HMS were reported by Prub et al. [30] for aerial oxidation of styrene with styrene oxide selectivity up to 44% and styrene conversion of 98%.

Zeolites are microporous crystalline aluminosilicate solids with well-defined channels and cavities having window diameters <1 nm. The aluminosilicate framework is negatively charged and is neutralised by extra-framework cations. Zeolite framework is sufficiently open to accommodate molecules and ions. Therefore, zeolites have been widely used and studied as ion exchangers, sorbents, and catalysts in industrial processes [31]. The extra-framework cations present in zeolites play a significant role in determining their adsorption and catalytic properties [32]. Zeolite X is a synthetic aluminium-rich analogue of the naturally occurring mineral faujasite (Fig. 1). The 14-hedron with 24 vertices known as the sodalite cavity or  $\beta$ -cage may be viewed as its principal building block. These  $\beta$ -cages are connected tetrahedrally at six-rings by bridging oxygen to give double six-rings (D6Rs, hexagonal prisms), and, concomitantly, an interconnected set of even larger cavities (supercage) accessible in three dimensions through 12-ring (24-membered) windows. The Si and Al atoms occupy the vertices of these polyhedra. The oxygen atoms lie approximately midway between each pair of Si and Al atoms but are displaced from those points to give near-tetrahedral angles about Si and Al. Single six-rings (S6Rs) are shared by sodalite and supercage and may be viewed as the entrances to the sodalite units. Each unit cell has eight sodalite units, eight supercage, 16 D6Rs, 16 12-rings, and 32 S6Rs. Exchangeable cations that balance the negative charge of the aluminosilicate framework are found

within the zeolite cavities. They are usually found at the six different sites: site I at the center of the D6R, I' in the sodalite cavity on the opposite side of one of the D6Rs six-rings from site I, II' inside the sodalite cavity near a S6R, II at the center of the S6R or displaced from this point into a supercage, III in the supercage on a twofold axis opposite a four-ring between two 12-rings, and III' somewhat or substantially off III (off the twofold axis) on the inner surface of the supercage.

The zeolites with transition metal ions as extra-framework cations have potential [31–34] to show novel catalytic behaviour as these cations are coordinately unsaturated, possess variable oxidation states and can form complexes with guest molecules more selectively than filled shell cations. Recently,  $\text{Co}^{2+}$ - and  $\text{Fe}^{2+}$ - [35] exchanged faujasite-type zeolites are reported to catalyse the epoxidation of styrene with  $\text{O}_2$  in the absence of a co-reductant. The highest styrene conversion of 46% with maximum epoxide selectivity 63% was reported in both the studies.

The present work was undertaken with an objective to develop a reusable solid catalyst for the epoxidation of styrene with higher styrene conversion and styrene oxide selectivity using molecular oxygen as oxidant. To achieve this, cobalt-exchanged zeolite X catalyst reported by Tang et al. [35] was further modified by increasing the cobalt content of the zeolite as well as introducing alkali and alkaline earth metal co-cations in the zeolite [36]. The effect of water molecules in the reaction system on the conversion of styrene to styrene oxide was also studied.

## 2. Experimental

### 2.1. Materials

Zeolite X was procured from Zeolites and Allied Products, Bombay, India. Unit cell chemical formula for the zeolite NaX was  $\text{Na}_{88}\text{Al}_{88}\text{Si}_{104}\text{O}_{384}$ , with unit cell dimension of 24.94 Å. The BET surface area of the NaX was 542  $\text{m}^2/\text{g}$ . Cobalt nitrate hexahydrate, potassium chloride, cesium chloride, magnesium chloride hexahydrate, calcium chloride dihydrate, strontium chloride hexahydrate, and barium chloride dihydrate were purchased from s. d. Fine Chemicals Ltd., Bombay, India. Chemical compositions of all the catalysts with structural and textural characteristics are given in Table 1. The number in the name of the catalyst denotes the percentage of sodium exchanged with cobalt in the zeolite. Styrene (99%) from Sigma-Aldrich, *N,N*-dimethylformamide (99.7%) from Qualigens Fine Chemicals Ltd., Bombay, India and oxygen (99.9%) from Inox Air Products Ltd., Bombay, India were used during the epoxidation studies.

### 2.2. Cation exchange

The sodium cations of the commercial zeolite X were replaced with various alkali and alkaline earth metal cations by ion exchange with potassium, rubidium, cesium, magnesium, calcium, strontium, and barium salt solution at 353 K separately or in combination. The ion-exchange process was repeated several times to achieve the higher replacement of sodium ions

Table 1  
Chemical composition and other characteristics of the catalysts used

Catalyst sample	Chemical composition (on dry basis)	Crystallinity (%)	BET surface area (m <sup>2</sup> g <sup>-1</sup> )	Micropore volume (cm <sup>3</sup> g <sup>-1</sup> )	External surface area (m <sup>2</sup> g <sup>-1</sup> )
NaX	Na <sub>88</sub> Al <sub>88</sub> Si <sub>104</sub> O <sub>384</sub>	100	508	0.217	44
NaCoX10	Co <sub>4.5</sub> Na <sub>79</sub> Al <sub>88</sub> Si <sub>104</sub> O <sub>384</sub>	98	549	0.235	44
NaCoX19	Co <sub>8.5</sub> Na <sub>71</sub> Al <sub>88</sub> Si <sub>104</sub> O <sub>384</sub>	94	556	0.236	47
NaCoX34	Co <sub>15</sub> Na <sub>58</sub> Al <sub>88</sub> Si <sub>104</sub> O <sub>384</sub>	92	619	0.266	51
NaCoX69	Co <sub>30.5</sub> Na <sub>27</sub> Al <sub>88</sub> Si <sub>104</sub> O <sub>384</sub>	84	640	0.269	64
NaCoX81	Co <sub>35.5</sub> Na <sub>17</sub> Al <sub>88</sub> Si <sub>104</sub> O <sub>384</sub>	80	652	0.274	52
NaCoX92	Co <sub>40.5</sub> Na <sub>7</sub> Al <sub>88</sub> Si <sub>104</sub> O <sub>384</sub>	74	676	0.286	52
NaCoX96	Co <sub>42.5</sub> Na <sub>3</sub> Al <sub>88</sub> Si <sub>104</sub> O <sub>384</sub>	72	676	0.289	55
KCoX19	Co <sub>8.4</sub> Na <sub>2.2</sub> K <sub>69</sub> Al <sub>88</sub> Si <sub>104</sub> O <sub>384</sub>	93	558	0.245	31
RbCoX22	Co <sub>9.7</sub> Na <sub>14.4</sub> Rb <sub>54.2</sub> Al <sub>88</sub> Si <sub>104</sub> O <sub>384</sub>	88	554	0.239	39
CsCoX20	Co <sub>8.8</sub> Na <sub>20.6</sub> Cs <sub>49.8</sub> Al <sub>88</sub> Si <sub>104</sub> O <sub>384</sub>	83	518	0.217	52
MgCoX22	Co <sub>9.7</sub> Na <sub>7.2</sub> Mg <sub>30.7</sub> Al <sub>88</sub> Si <sub>104</sub> O <sub>384</sub>	92	668	0.282	60
CaCoX19	Co <sub>8.4</sub> Na <sub>4</sub> Ca <sub>33.6</sub> Al <sub>88</sub> Si <sub>104</sub> O <sub>384</sub>	93	567	0.244	45
SrCoX18	Co <sub>7.9</sub> Na <sub>5</sub> Sr <sub>33.6</sub> Al <sub>88</sub> Si <sub>104</sub> O <sub>384</sub>	93	326	0.139	26
BaCoX15	Co <sub>6.6</sub> Na <sub>5.6</sub> Ba <sub>34.6</sub> Al <sub>88</sub> Si <sub>104</sub> O <sub>384</sub>	90	407	0.171	39
CsBaCoX20	Co <sub>8.8</sub> Na <sub>9.2</sub> Cs <sub>28</sub> Ba <sub>16.6</sub> Al <sub>88</sub> Si <sub>104</sub> O <sub>384</sub>	83	432	0.182	41
KBaCoX21	Co <sub>9.2</sub> Na <sub>2.2</sub> K <sub>34</sub> Ba <sub>16.7</sub> Al <sub>88</sub> Si <sub>104</sub> O <sub>384</sub>	91	415	0.179	29
KSrCoX20	Co <sub>8.8</sub> Na <sub>2.4</sub> K <sub>37</sub> Sr <sub>15.5</sub> Al <sub>88</sub> Si <sub>104</sub> O <sub>384</sub>	90	256	0.110	20

with other alkali and alkaline earth metals. Cobalt cations were introduced into highly crystalline zeolite X by the cobalt ion exchange from aqueous solution. Typically, the zeolite was treated with 0.05 M aqueous solution of the cobalt nitrate at a solid/liquid ratio 1:80 at 353 K for 4 h. The residue was filtered and washed with hot distilled water, until the washing was free from nitrate ions and dried in air at room temperature. Zeolite X samples with varying amounts of cobalt exchange were prepared by repeated ion exchanges of the commercial zeolite. The extent of cobalt exchange in zeolite X was determined by the complexometric titration of the original solution and filtrate obtained after the ion exchange with EDTA using a murexide indicator.

### 2.3. Catalytic characterization

X-ray powder diffraction measurements of various cobalt-exchanged zeolite X at ambient temperature were carried out using a PHILIPS X'pert MPD system in the  $2\theta$  range of 5°–65° using CuK $\alpha$  ( $\lambda = 1.54056$  Å). The diffraction pattern of the starting material demonstrates that it is highly crystalline, showing reflections at  $2\theta$  values 6.1°, 10.0°, 15.5°, 20.1°, 23.4°, 26.7°, 29.3°, 30.5°, 31.0°, and 32° in the range of 5°–35° typical of zeolite X. The percent crystallinity of the cobalt ion-exchanged zeolites was determined from the X-ray diffraction pattern by summing the intensities of 10 major peaks.

Surface area and pore size distribution of the various cobalt-exchanged zeolites were determined from the N<sub>2</sub> adsorption data at 77.35 K. The equilibrium nitrogen adsorption at 77.35 K was measured using a Micromeritics ASAP 2010. The samples were activated at 373 K under vacuum ( $5 \times 10^{-3}$  mm Hg) for 12 h before the N<sub>2</sub> sorption measurements. The surface areas of different catalyst samples were determined by applying the BET equation to the measured N<sub>2</sub> adsorption data. Micropore volume and external area were determined from  $t$  plots of the data.

Diffuse reflectance spectroscopy (DRS) studies were performed with a Shimadzu UV-3101PC equipped with an integrating sphere. BaSO<sub>4</sub> was used as the reference material. The spectra were recorded at room temperature in the wavelength range of 200–750 nm.

### 2.4. Catalytic epoxidation reactions

The cobalt ion-exchanged zeolites dried at room temperature were used for the catalytic studies with no further activation. The catalytic epoxidation reactions were carried out in liquid phase as a batch reaction at 373 K. Typically, a 50-ml round-bottomed flask equipped with an efficient water condenser is kept in a constant temperature oil bath with the temperature maintained at  $373 \pm 2$  K. Then 10 mmol styrene along with 20 ml of *N,N*-dimethylformamide (DMF) and 200 mg of catalyst were added to the flask. The reaction was started by bubbling O<sub>2</sub> at atmospheric pressure into the reaction mixture at the rate of 6–8 ml min<sup>-1</sup>. Tridecane was used as an internal standard. The reaction mixture was magnetically stirred at 600 rpm. After 4 h of reaction, the catalyst was separated by centrifuging the reaction mixture, and the liquid organic products were quantified using a gas chromatograph (Hewlett-Packard model 6890) equipped with a flame ionisation detector and an HP-5 capillary column (30 m long and 0.32 mm in diameter, packed with silica-based supel cosil), a programmed oven (temperature range 348–493 K), and N<sub>2</sub> as the carrier gas. Gas chromatograph–mass spectrometer (GC–MS), analysis using a Shimadzu GCMS-QP-2010, was done with the GC oven programmed at the temperature range of 348–493 K and helium as the carrier gas and MS in the EI mode with a 70-eV ion source. The reaction kinetics were monitored by carefully withdrawing small amounts of the reaction liquid with a microsyringe from the reaction flask, avoiding solid catalyst, at 30-min intervals and analysing its composition by GC. Calibration of GC peak areas of styrene and styrene oxide was done using solu-

tions with known amounts of styrene and styrene oxide in DMF. The conversion was calculated on the basis of molar percent of styrene; the initial molar percent of styrene was divided by initial area percent (styrene peak area from GC) to get the response factor. The unreacted moles of styrene remaining in the reaction mixture were calculated by multiplying the response factor by the area percentage of the GC peak for styrene obtained after the reaction. The conversion, selectivity, and turnover frequency (TOF) were calculated as follows:

$$\text{conversion (mol\%)} = \frac{(\text{initial mol\%}) - (\text{final mol\%})}{\text{initial mol\%}} \times 100, \quad (1)$$

$$\text{styrene oxide selectivity} = \frac{\text{GC peak area of styrene oxide}}{\text{GC peak area of all products}} \times 100, \quad (2)$$

$$\text{TOF} = \frac{\text{No. of moles of styrene oxide formed}}{\text{No. of moles of cobalt in the catalyst} \times \text{reaction time}}. \quad (3)$$

### 2.5. Catalyst regeneration

The spent catalyst was recovered from the reaction mixture by filtration and thoroughly washed with DMF and distilled water, then dried in air at room temperature.

### 2.6. Isothermic heat of adsorption

Isothermic heats of adsorption of oxygen on various catalysts were calculated by the Clausius–Clapeyron equation from the oxygen adsorption data measured at 288.2 and 303.0 K using a static volumetric system (Micromeritics model ASAP 2010). The details of the adsorption isotherm measurement have been described elsewhere [37]. The samples were activated in situ by increasing the temperature from room temperature to 673 K under vacuum ( $5 \times 10^{-3}$  mmHg) for 8 h before the adsorption measurements. The adsorption temperature was maintained ( $\pm 0.1$  K) by circulating water from a constant temperature bath (Julabo F25). A requisite amount of the adsorbate gas was injected into the volumetric setup at volumes required to achieve a targeted set of pressures ranging from 0.1 to 850 mm Hg. Isothermic heat of adsorption,

$$-\Delta H = R \left[ \frac{\partial \ln P}{\partial (1/T)} \right]_{\theta}, \quad (4)$$

where  $R$  is the universal gas constant,  $\theta$  is the fraction of the adsorbed sites at a pressure  $P$  and temperature  $T$ . Error in the heat of adsorption was estimated to be 0.4%.

## 3. Results and discussion

Complete  $\text{Co}^{2+}$  exchange of NaX was attempted from aqueous solution at 353 K, but the maximum  $\text{Na}^+$  ion exchange with  $\text{Co}^{2+}$  that could be achieved was 96%. The overall structure of the zeolite X was retained during the cation-exchange process, as demonstrated by the presence of all the major reflections. However, zeolite samples with higher cobalt content

(NaCoX69, NaCoX81, NaCoX92, and NaCoX96) showed decreased crystallinity. Decreased crystallinity was also observed for zeolite samples with lower cobalt content but with cesium and barium as co-cations. This observed decrease could be due to structural deformation occurring during exchange of large-sized cesium and barium cations into the zeolite structure or interaction of  $\text{Co}^{2+}$  cations with framework oxygen of zeolite.

BET surface area, micropore volume, and external surface area were calculated by fitting the adsorption data in the corresponding theories; the values are given in Table 1. The surface area of the zeolite X samples was observed to increase on cobalt ion exchange. This is due to the decrease in the number of extra-framework cations while replacing monovalent sodium ions with divalent cobalt ions. On replacing sodium ions with divalent cations such as cobalt, one  $\text{Co}^{2+}$  replaces two  $\text{Na}^+$  ions; therefore, half of the cations are present in the zeolite. The external surface area determined from the  $t$ -plot also increases with the percentage of cobalt exchange. This can be explained in terms of the structural deformation occurring during the cation-exchange process and/or vacuum dehydration at higher temperatures, which is also apparent from the decreased crystallinity. The large decrease in surface observed for  $\text{K}^+$ ,  $\text{Ba}^{2+}$ ,  $\text{Sr}^{2+}$ , and  $\text{Cs}^+$  ion-exchanged zeolites is due to the large cation size of these ions compared with  $\text{Na}^+$  ions.

In the hydrated pink sample, NaCoX, spectral minima appeared around 530 nm in the visible region and 240 nm in the UV region (Fig. 2), which are assigned to the transitions of the octahedral  $[\text{Co}(\text{H}_2\text{O})_6]^{2+}$  complex located in the supercages of the zeolite X [38]. Fig. 2 also shows that for zeolite samples with Co exchange >60%, a band appeared at around 620 nm, indicating the presence of tetrahedral coordination of Co(II). UV-vis DRS spectra of various Co(II)X samples with co-cations in the presence of DMF are given in Fig. 3. These spectra show that the peaks became broader and the maxima was shifted to higher wavelengths with increasing intensity in the presence of DMF solvent. However, in the presence of DMF, even with ca. 20% cobalt exchange in zeolite, the colour shifted to violet, demonstrating the changed coordination environment from octahedral cobalt to tetrahedral coordination in the presence of DMF.

### 3.1. Epoxidation of styrene to styrene oxide using molecular oxygen

Styrene was converted into styrene oxide at 373 K with molecular oxygen in DMF using cobalt-exchanged zeolite X as catalyst. Styrene oxide and benzaldehyde were formed as the major products, as confirmed by GC–MS of the reaction products. The mass data showed standard fragmentation patterns corresponding to styrene epoxide ( $m/z = 120, 91, 65, 51$ ) and benzaldehyde ( $m/z = 106, 77, 51$ ), which were the products formed in the reaction.

The catalytic activity of various catalysts with different amounts of cobalt ion-exchanged zeolite X toward the epoxidation reaction of styrene was determined by the reaction between molecular oxygen and styrene at 373 K in the presence of these catalysts. A 200-mg catalyst sample was used in all of

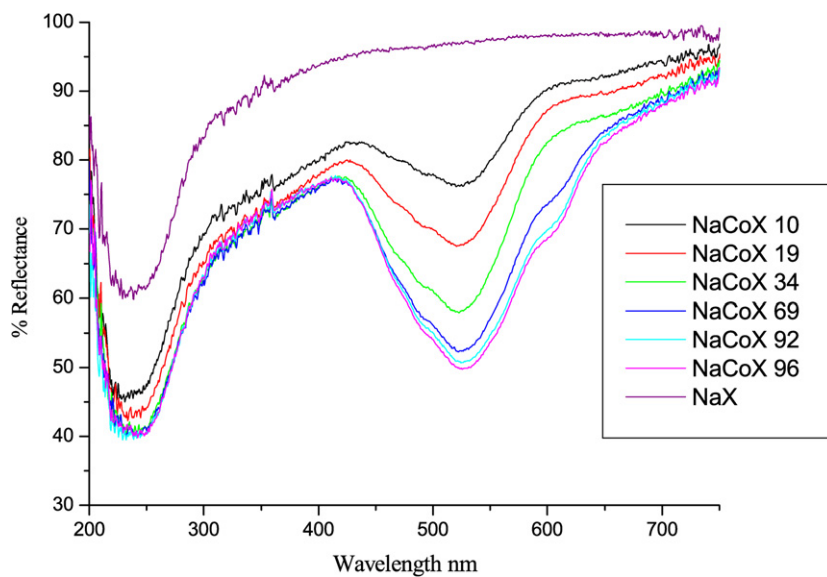


Fig. 2. Diffuse reflectance spectra of various amounts of cobalt(II) ion-exchanged zeolite X.

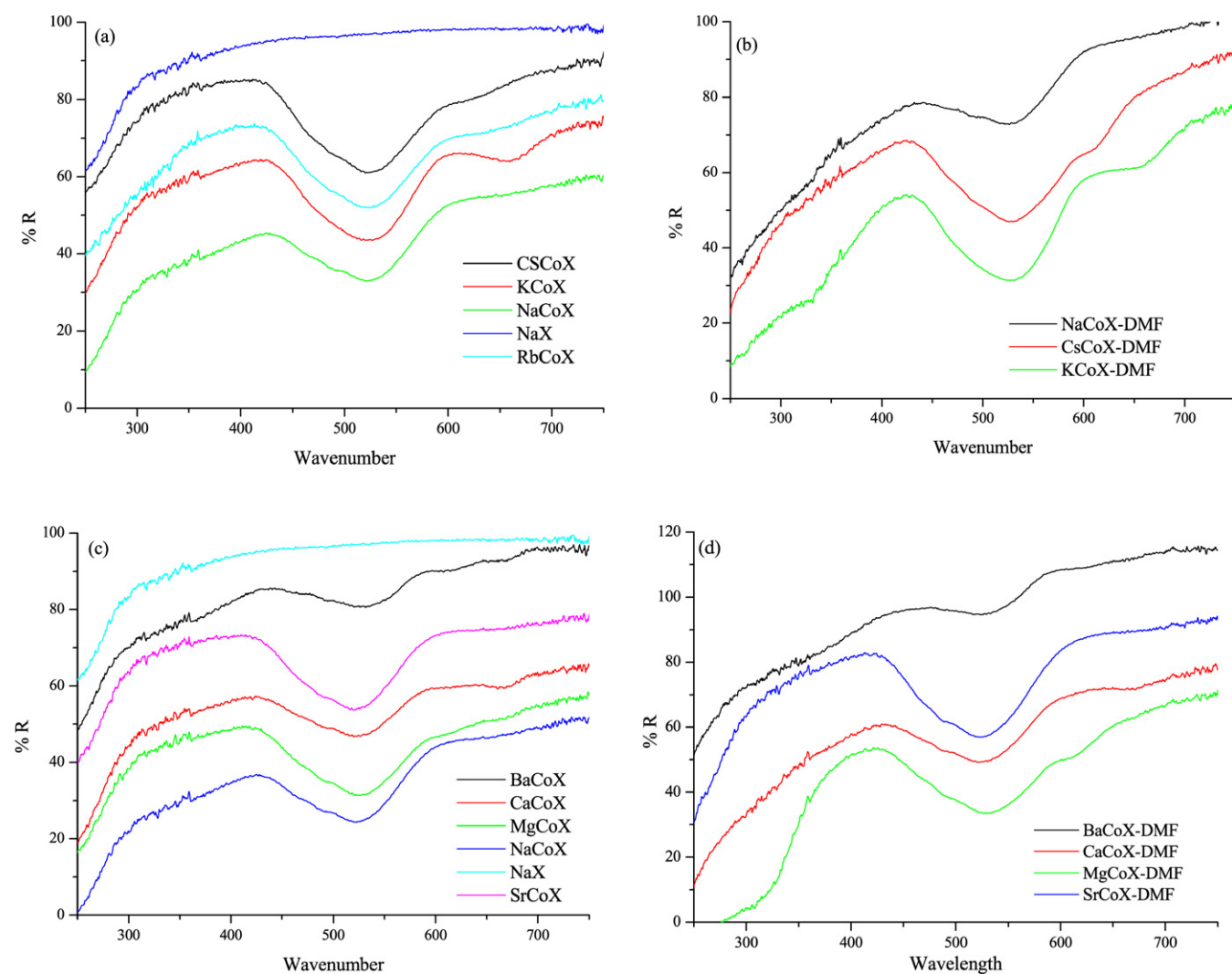


Fig. 3. DRS spectra of (a) alkali metal-exchanged CoX, (b) DMF adsorbed alkali metal-exchanged CoX, (c) alkaline earth metal-exchanged CoX and (d) DMF adsorbed alkaline earth metal-exchanged CoX.

Table 2  
Performance of NaCoX catalysts in styrene epoxidation<sup>a</sup>

Entry	Catalyst	Conversion of styrene (%)	Selectivity of styrene oxide (%)	Selectivity of benzaldehyde (%)	TOF (h <sup>-1</sup> )
1	NaX	3	57	43	–
2	NaCoX10	66	67	33	25.3
3	NaCoX19	78	68	32	15.9
4	NaCoX34	88	65	35	9.7
5	NaCoX69	97	68	32	5.6
6	NaCoX81	98	68	32	4.8
7	NaCoX92	98	66	34	4.2
8	NaCoX96	100	67	33	4.1
9	NaCoX92 <sup>b</sup>	99	66	34	4.2
10	NaCoX96 <sup>b</sup>	99	66	34	4.0

<sup>a</sup> Reaction conditions: Styrene = 10 mmol; DMF = 20 ml; catalyst = 200 mg; O<sub>2</sub> ≅ 6–8 ml min<sup>-1</sup>; duration = 4 h.

<sup>b</sup> Air ≅ 10 ml min<sup>-1</sup> was used instead of oxygen.

the reactions independent of the extent of cobalt exchange. Catalysts air-dried at room temperature after the cation-exchange processes were used for the epoxidation reactions without any thermal treatment or activation. The percentage conversion and selectivity obtained for different cobalt-exchanged zeolites are given in Table 2. The table shows that the styrene conversion increased sharply on exchanging the zeolite X the extra-framework cations with cobalt ions and further increased with increasing cobalt content. Some 66% of the styrene conversion occurred during the 4 h of reaction time using NaCoX containing 10% cobalt ions. The styrene conversion exceeded 97% when the cobalt exchange was increased to 69%. Styrene oxide selectivity also increased on cobalt exchange, from 56% in NaX to 66% in NaCoX10, but the selectivity remained almost unaffected with further increases in the amount of cobalt ions in the zeolite. This increased styrene conversion at higher cobalt-exchange levels may be due to the occupation of the cobalt ions in the more accessible locations in the zeolite structure.

The crystal structure of cobalt-exchanged zeolite X reported in the literature [4] show that the Co<sup>2+</sup> ions prefer site II. After completely occupying the available site II locations, Co<sup>2+</sup> ions occupied sites I' and III'. The cations in site I' were not accessible to the oxygen molecules. The cations in site II could interact with the oxygen molecules through the six-member ring windows, and the cations in site III' could interact directly with oxygen. The distances between the Co<sup>2+</sup> ions in site III' and the framework oxygen atoms are long (Co–O distances of 2.30 and 2.27 Å), and these Co<sup>2+</sup> ions were relatively coordinately unsaturated compared with the Co<sup>2+</sup> cations present in site II, wherein Co–O distance is 2.129 Å. Therefore, cobalt cations present in site III' would be expected to be catalytically more active for the activation of the oxygen molecules for the styrene epoxidation reaction compared with the cobalt cations present in site II.

TOF values were decreased with increasing amounts of cobalt in the zeolite. This may be due to the fact that at higher cobalt-exchange levels, some of the cobalt ions may move to the cation locations inside the sodalite cavities, making them inaccessible to the oxygen molecules, or due to the occupancy of the cobalt ions in the neighbouring sites, making some of the cobalt sites inaccessible for the styrene epoxidation reaction. The increased styrene conversion and decreased TOF values with increasing cobalt exchange in NaX (Table 2) demonstrate that the number of catalytically active Co(II) species increased with increasing cobalt exchange, however, the percentage of such species decreased with increasing cobalt exchange in NaX.

### 3.2. Kinetics of styrene oxidation

The changes in the concentrations of styrene and styrene oxide relative to the concentration of the internal standard as a function of time are shown in Fig. 4 for NaCoX96. Styrene conversion and styrene oxide formation increased with time and

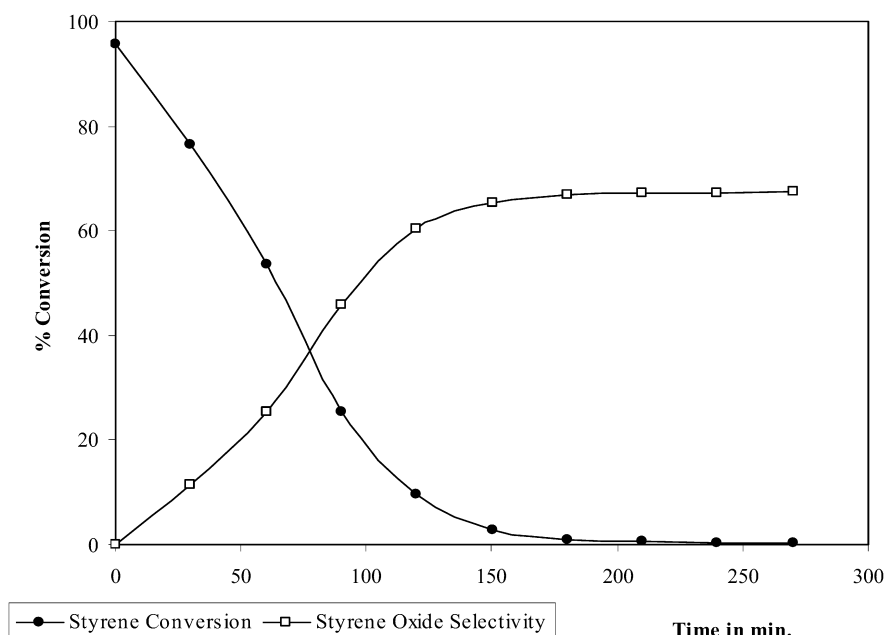


Fig. 4. Kinetics of styrene conversion and styrene oxide formation using NaCoX96.

reached near maximum at 210 min. An increase in reaction time up to 270 min did not effect the concentrations of either styrene or styrene oxide. However, further increases led to decreased styrene oxide concentration. The styrene oxide formed underwent ring-opening reactions, and such products as styrene glycol were formed. The rate constant of the epoxidation reaction was derived by applying the first-order rate equation [39] and was found to be  $0.02589 \text{ min}^{-1}$ .

### 3.3. Catalytic oxidation with air

Catalytic oxidation was also carried out using air as the molecular oxygen source. Instead of oxygen, air was bubbled into the reaction at a rate of  $10 \text{ ml min}^{-1}$ . Atmospheric air was bubbled into the reaction system without any purification or drying using an air pump (entries 9 and 10 in Table 2). The styrene conversion, styrene oxide selectivity, and TOF values were similar to those of the reactions carried out using chemically pure (99.9%) oxygen as the oxidant. The conversion, selectivity, and TOF values obtained are given in Table 2 and are comparable to the data obtained with pure oxygen.

### 3.4. Effect of water on the catalytic reaction

The effect of water in the reaction medium was explored by carrying out four reactions in which the reaction system contained different amount of water molecules. In the first reaction, the solvent was dried [60] and catalyst was also dehydrated at 353 K under vacuum ( $10^{-3}$  Torr) for 24 h. The styrene conversion was only 42%, with a styrene oxide selectivity of 68%. In the second reaction, the solvent was used without drying, and the catalyst was dehydrated at 353 K under vacuum ( $10^{-3}$  Torr) for 24 h. The styrene conversion increased (Table 3) to 65% with styrene oxide selectivity of 67%. The third reaction was carried out using the catalyst and solvent as obtained without any activation or drying. The styrene conversion increased to 98% with a styrene oxide selectivity of 66%. In the fourth reaction, 1.0 ml of water was added to the reaction system, and there was no significant effect on the styrene conversion and styrene oxide selectivity. The TOF also increased from 1.8 to 4.2 on in-

Table 3  
Effect of water on the catalytic activity using NaCoX92 catalyst<sup>a</sup>

Entry	Reaction system	Conversion of styrene (%)	Selectivity of styrene oxide (%)	TOF ( $\text{h}^{-1}$ )
1	DMF (dried) and catalyst activated at 353 K/vacuum ( $10^{-3}$ Torr)	42	68	1.8
2	DMF without drying and catalyst activated (353 K/vacuum, $10^{-3}$ Torr)	65	67	2.8
3	DMF without drying and catalyst unactivated	98	66	4.2
4	DMF without drying, catalyst unactivated and 1.0 ml H <sub>2</sub> O	100	65	4.2

<sup>a</sup> Reaction conditions: Styrene = 10 mmol; DMF = 20 ml; amount = 200 mg; O<sub>2</sub>  $\cong$  6–8 ml min<sup>-1</sup>; duration = 4 h.

creasing the amount of water in the reaction system. The same catalyst (NaCoX92) was used for the catalytic epoxidation reactions in all reactions. These data, given in Table 3, show that the presence of water in the catalyst/reaction medium affects styrene conversion. A similar increase in TOF was reported by Iliev et al. [40] during the oxidation of 2-mercaptoethanol to disulfide with oxygen using a Co(II) phthalocyanine complex in microporous hydrotalcite. The enhanced catalytic activity was attributed to improved dispersion of cobalt complex in the hydrotalcite host in the presence of DMF–water mixture [41]. The mechanism for the effect of water molecules on the catalytic epoxidation of styrene to styrene oxide with molecular oxygen using Co(II)-exchanged zeolite is not completely understood. However, it seems that the presence of the DMF–water mixture in zeolite X could result in the relocation of Co(II) ions so that more ions are present at sites that are catalytically active/accessible to substrate molecules. This is supported by the increased TOF values in the presence of the DMF–water mixture from 2.8 to 4.2 h<sup>-1</sup>.

### 3.5. Effect of alkali and alkaline earth metal cations on the reaction

The effect of alkali and alkaline earth metal cations on the catalytic epoxidation of styrene to styrene oxide with molecular oxygen using cobalt-exchanged zeolites was studied. The sodium ions of the zeolite were exchanged with K<sup>+</sup>, Rb<sup>+</sup>, Cs<sup>+</sup>, Mg<sup>2+</sup>, Ca<sup>2+</sup>, Sr<sup>2+</sup>, and Ba<sup>2+</sup> cations. In these ion-exchanged zeolites, ca. 20% of the extra-framework sodium cations were replaced with cobalt ions by ion exchange from aqueous solution. The catalytic properties of K<sup>+</sup>, Rb<sup>+</sup>, Cs<sup>+</sup>, Mg<sup>2+</sup>, Ca<sup>2+</sup>, Sr<sup>2+</sup>, and Ba<sup>2+</sup> cations containing CoX were determined under the same reaction conditions; the catalytic properties of these alkali and alkaline cations, including CoX samples, are compared in Table 4. The catalytic epoxidation of styrene to styrene oxide with molecular oxygen using cobalt-exchanged zeolite X

Table 4  
Styrene epoxidation using CoX having various alkali metal promoters<sup>a</sup>

Entry	Catalyst	Conversion of styrene (%)	Selectivity of styrene oxide (%)	Selectivity of benzaldehyde (%)	TOF ( $\text{h}^{-1}$ )
1	NaCoX19	78	68	32	15.9
2	KCoX19	99	71	29	22.7
3	RbCoX21	99	72	28	24.0
4	CsCoX20	100	77	23	26.4
5	MgCoX22	100	75	25	21.1
6	CaCoX19	100	83	17	24.9
7	SrCoX18	100	85	15	27.4
8	BaCoX15	100	83	17	32.5
9	CsBaCoX20	100	80	20	27.8
10	KBaCoX21	100	83	17	26.9
11	KSrCoX20	100	81	19	26.5
12	BaCoX15 <sup>b</sup>	93	66	34	–
13	BaCoX15 <sup>c</sup>	99	83	17	–

<sup>a</sup> Reaction conditions: Styrene = 10 mmol; DMF = 20 ml; catalyst = 200 mg; O<sub>2</sub>  $\cong$  6–8 ml min<sup>-1</sup>; duration = 4 h.

<sup>b</sup> 1,4-dioxane was used as solvent in place of DMF.

<sup>c</sup> DMA was used as solvent in place of DMF.

with alkali and alkaline metal ions showed increased selectivity of styrene oxide while moving down the periodic table. Styrene conversion increased from 78% in NaCoX to 99% in KCoX, RbCoX, and CsCoX. Styrene oxide selectivity also increased, from 68% in NaCoX to 71% in KCoX, 72% in RbCoX, and 77% in CsCoX (entries 1–4 in Table 4). In addition, TOF values increased from 15.9 to 22.7, 24.0, and 26.4 on replacing the sodium ions of CoX with potassium, rubidium, and cesium, respectively.

Similarly, styrene conversion was >99% with all of the Co(II)-exchanged zeolite X catalysts with alkaline earth metal cationic promoters. The styrene oxide selectivity also increased from 68% in NaCoX to 75% in MgCoX, 83% in CaCoX, 85% in SrCoX, and 83% in BaCoX (entries 1 and 5–8 in Table 4). TOF increased from 15.9 to 21.1, 24.9, 27.4, and 32.5 on replacing the sodium ions of CoX with magnesium, calcium, strontium, and barium, respectively. The increased styrene epoxide selectivity for CoX with alkaline earth metal ions was higher than that for CoX with alkali metal cation ions.

The effect of a mixture of alkali–alkaline earth metal cations on the catalytic epoxidation of styrene to styrene oxide with molecular oxygen using cobalt-exchanged zeolites was also studied. The sodium ions of the zeolite were exchanged with a mixture of alkali–alkaline earth metal cations such as K<sup>+</sup>, Cs<sup>+</sup>, Sr<sup>2+</sup>, and Ba<sup>2+</sup>. Approximately 20% of the extra-framework cations of these zeolites were replaced with cobalt ions by ion exchange from aqueous solution. The catalytic activities of the three catalysts are compared in Table 4.

Three alkali–alkaline earth metal cationic combinations were studied: CsBaCoX, KBaCoX, and KSrCoX (entries 9–11 in Table 4). Styrene conversions and styrene oxide selectivities were very high (>99 and >80%, respectively, in all cases) compared with the values for the corresponding NaCoX. TOF values were also high in these CoX-containing mixed cationic promoters.

### 3.6. Reactions using spent catalysts

Catalysts were recovered from the reaction mixture by centrifuging, and the recovered catalyst was washed with DMF and then with distilled water to remove all of the organic phases adsorbed on the catalyst. The conversion and selectivity obtained at the second and third cycles are given in Table 5. The numbers in roman letters denote the reaction cycle numbers using the same catalyst. As seen from the data, the catalytic activity of the catalysts remained unaffected after two or three reaction cycles.

The analysis of the liquid phase separated from the reaction mixture did not show the presence of cobalt cations in solution, indicating the absence of leaching of the cobalt metal ions during the catalytic reaction. The cobalt(II) cations present in the zeolite had a strong interaction with the zeolite framework. The interactions between the cations and the zeolite framework were strong enough to keep the cations intact with the zeolite structure under the reaction and activation conditions used in the catalytic reaction.

Table 5  
Performance of spent MCoX catalysts in styrene epoxidation<sup>a</sup>

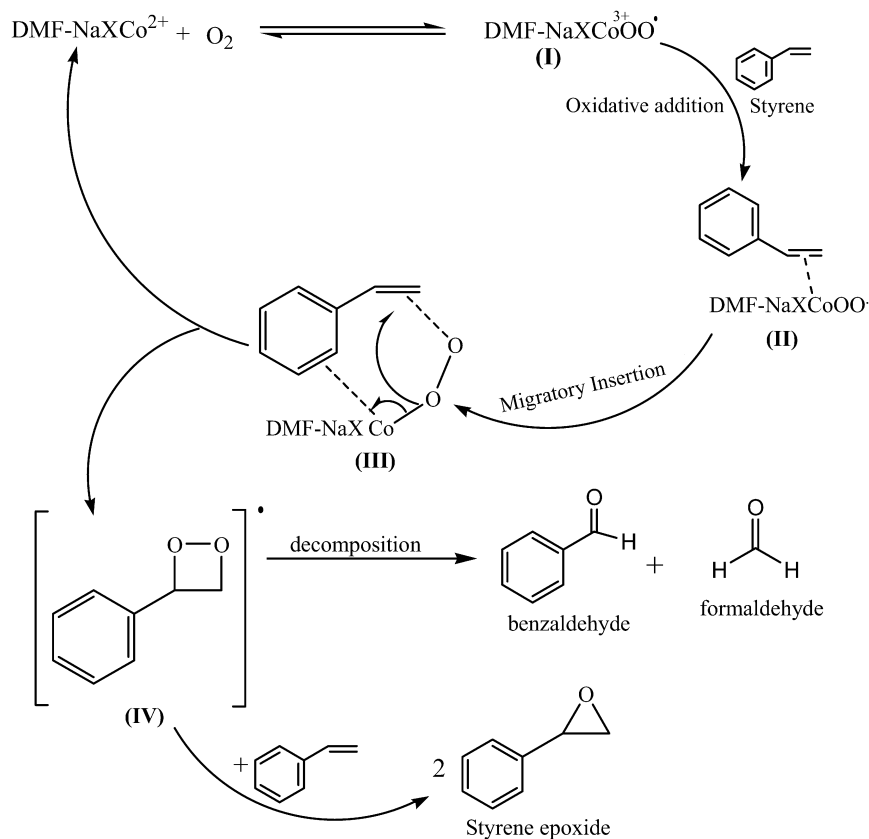
Entry	Catalyst	Conversion of styrene (%)	Selectivity of styrene oxide (%)	Selectivity of benzaldehyde (%)	TOF (h <sup>-1</sup> )
1	NaCoX92 I	98	66	34	4.2
2	NaCoX92 II	99	67	33	4.3
3	NaCoX92 III	99	67	33	4.2
4	NaCoX96 I	100	67	33	4.1
5	NaCoX96 II	100	66	34	4.0
6	NaCoX96 III	100	66	34	4.0
7	KCoX19 I	99	71	29	22.7
8	KCoX19 II	99	72	28	23.0
9	CsCoX20 I	100	77	23	26.4
10	CsCoX20 II	100	77	23	26.4
11	SrCoX18 I	100	85	15	27.4
12	SrCoX18 II	100	85	15	27.5
13	BaCoX15 I	100	83	17	32.5
14	BaCoX15 II	100	83	17	32.5

<sup>a</sup> Reaction conditions: Styrene = 10 mmol; DMF = 20 ml; catalyst = 200 mg; O<sub>2</sub> ≅ 6–8 ml min<sup>-1</sup>; duration = 4 h.

### 3.7. Reaction mechanism

The data on conversion, selectivity, TOF, and activity of the spent catalyst show that the cobalt-exchanged zeolites X with alkali and alkaline earth metal ions are potential catalysts in the catalytic epoxidation of styrene to styrene oxide using molecular oxygen. Our findings confirm that alkaline earth metal cations are more effective co-cations than alkali metal cations for enhancing styrene epoxide selectivity when exchanged into zeolite X with cobalt ions. It is interesting to note that in alkali and alkaline earth-exchanged cations, <20% cobalt exchange is needed to obtain 98–99% styrene conversion, improved styrene epoxide selectivity, and higher TOF values. To study the mechanistic behaviour and also to identify the active species formed in the experiment, a small amount of free radical scavenger hydroquinone (50 mg) was added, and catalytic activity with NaCoX92 was studied. Under the same reaction conditions specified in Table 2, the conversion of styrene to styrene oxide was found to be almost zero. This finding, along with earlier results of Tang et al. [35], confirm that formation of free-radical-type active oxygen species occurs, probably due to activation of O<sub>2</sub> in the Co<sup>2+</sup> cations present at site III' or II. It is well known [35,42–47] that many cobalt(II) complexes can bind and activate oxygen-forming Co(III)–(O<sub>2</sub><sup>-</sup>) species, which further undergo reactions to generate peroxy and superoxy radical-type active oxygens. The UV–vis spectra observed by us and reported by Tang et al. [35] indicate that Co(II) ions present in zeolite X are in tetrahedral coordination in the presence of DMF. Furthermore, based on the observation of a C=O stretching shift of free DMF from 1671 to 1658 cm<sup>-1</sup> in the presence of NaCoX in the FTIR spectra of a Co(II)–NaX–DMF adduct, it has been reported [34] that DMF molecules are coordinated to the cobalt cations present in the zeolite supercage through oxygen atoms of DMF. This is further supported by the experimental data measured with three solvents (entries 12 and 13 in Table 4). Higher conversion and epoxide selectivity was observed for solvents with carbonyl groups DMA and DMF





Scheme 1. Proposed tentative reaction mechanism for the epoxidation of styrene.

compared with 1,4-dioxane. It is also known that DMF has a higher oxygen-dissolving capacity than other solvent media. The mechanism of catalytic epoxidation of styrene to styrene oxide with molecular oxygen using Co(II)-exchanged zeolite is not completely understood; however, we propose a tentative mechanism (Scheme 1) based on that proposed by Pruß et al. [34] and that reported for cobalt complexes in homogeneous media. We believe that Co(II)NaX-DMF present in the zeolite supercage is coordinated to molecular oxygen to form a DMF-NaXCo(III)OO·(I) superoxo type of complex, resulting in oxidative addition to the C=C double bond of styrene molecules to give an intermediate (II). The intermediate (II) undergoes migratory insertion to give cyclic peroxide radical (III) and regenerates DMF-NaXCo(II). Cyclic peroxide radical (IV) can further react with another molecule of styrene to give styrene epoxide or can undergo thermal decomposition to benzaldehyde and formaldehyde. The observation that styrene epoxide selectivity increases as the basicity of zeolite increases for various alkali and alkaline earth cation exchanges can be explained in terms of the higher stabilization of intermediate (III) radical with increased basicity, which will decrease its decomposition to benzaldehyde and formaldehyde, thereby giving higher selectivity for epoxide. As the reaction is carried out at 100 °C under oxygen flow, the formaldehyde formed escapes along with oxygen and cannot be detected in the reaction products by GC or GC-MS analysis. Therefore, to confirm the formation of formaldehyde, a separate styrene epoxidation experiment as described in the following section was carried out.

Here, 10 mmol styrene along with 20 ml of DMF and 200 mg of SrCoX18 catalyst were added to a 50-ml round-bottomed flask equipped with an efficient water condenser that was placed in an oil bath, with the temperature maintained at  $373 \pm 2$  K. The reaction was started by bubbling  $\text{O}_2$  at atmospheric pressure into the reaction mixture at the rate of  $6\text{--}8$  ml  $\text{min}^{-1}$ . The reaction mixture was magnetically stirred at 600 rpm. An outlet was provided at the top of the condenser using tubing into a beaker containing 15 ml of distilled water so that vapours formed during the reaction were carried by the purged oxygen and became dissolved in it. After 4 h of reaction, 1 ml of water containing the dissolved vapours was placed in the test tube, and a small amount of resorcinol and 5–6 drops of conc.  $\text{H}_2\text{SO}_4$  were added. At the junction of the two liquids, a clear red ring formation was observed, along with white precipitate in the aqueous layer, which changed to violet-red after standing, clearly confirming the presence of formaldehyde.

The stability of the radicals in zeolite pores is reportedly related to the basicity of the framework oxygen of alkali-exchanged zeolites [48–54], indicating that increased basicity leads to higher radical stability. The basicity of alkali cation-exchanged zeolite increases in the order  $\text{Cs-X} > \text{Rb-X} > \text{K-X} > \text{Na-X}$  as determined by IR [55] and XPS studies [56]. The values of the partial negative charge on oxygen as a function of energy calculated from the blue shift of adsorbed iodine in relation to gaseous iodine showed a similar trend [57]. We calculated the average partial charges on oxygen atoms using Sanderson electronegativity methods [58] and found values of

Table 6  
Isosteric heat of adsorption for oxygen on various CoX catalysts

Catalyst	Isosteric heat of adsorption (O <sub>2</sub> ) in kJ mol <sup>-1</sup>
NaX	15.1
NaCoX10	15.9
NaCoX19	16.4
NaCoX34	16.9
NaCoX69	17.4
NaCoX81	17.9
NaCoX92	18.3
NaCoX96	18.5
KCoX19	17.2
RbCoX21	17.4
CsCoX20	17.5
MgCoX22	17.6
CaCoX19	18.5
SrCoX18	18.7
BaCoX15	18.9

–0.34 for CsCoX20, –0.32 for RbCoX21, –0.31 for KCoX19, and –0.30 for NaCoX19. Similarly, the basicity of alkaline earth cation-exchanged zeolites increased as we go down the group, as demonstrated by the average partial charges on oxygen atoms of –0.25 for BaCoX15, –0.24 for SrCoX18, –0.23 for CaCoX19, and –0.22 for MgCoX22. Similar effects of alkali and alkaline earth metal cations were observed for the kinetics of ammonia synthesis catalysed by ruthenium supported on zeolite X and the selective oxidation of butane by nickel molybdate with oxygen [59].

Alkali and alkaline cations can also enhance the catalytic epoxidation reaction of styrene to styrene oxide through relocation/dispersion of the cobalt ions inside the zeolite pores to catalytically more active locations. The observation of significantly increased TOF in the presence of alkali/alkaline cations with even 20% cobalt exchange demonstrates the greater amount of Co(II) compared with NaCoX20 at catalytically active sites in these samples. The isosteric heat of adsorption (Table 6) for oxygen molecules increased from 15.1 kJ mol<sup>-1</sup> in NaX to 18.5 kJ mol<sup>-1</sup> in NaCoX96. Table 6 clearly shows that the isosteric heat of adsorption for oxygen molecules increases with increasing cobalt content of the zeolite X. This clearly indicates the stronger interaction of the oxygen molecules with the Co(II) cations present in the zeolite X. Co(II)-exchanged zeolite X catalysts with potassium, rubidium, and cesium cationic promoters demonstrated increased oxygen heat of adsorption values. The oxygen heat of adsorption values in the Co(II)-exchanged zeolite X catalysts with magnesium, calcium, strontium, and barium cationic promoters were significantly higher than those in NaCoX with similar cobalt content. The oxygen heat of adsorption values in these zeolites containing only ca. 20% cobalt ions were similar to those in NaCoX96.

#### 4. Conclusion

An eco-friendly and efficient catalytic system comprising Co<sup>2+</sup>-exchanged faujasite zeolites has been studied for liquid-phase epoxidation of styrene using molecular oxygen. A 100% conversion of styrene with 65% styrene oxide selectivity was

achieved using NaCoX. The effect of water concentration on the reaction system was studied. Alkali and alkaline earth cationic promoters were introduced into the zeolite to enhance the activity of the catalyst. The styrene oxide selectivity increased on replacing the sodium ions with higher alkali metal cations, from 68% for NaCoX to 77% for CsCoX. The styrene oxide selectivity also increased on replacing the sodium ions with alkaline earth metal cations; a maximum styrene oxide selectivity of 85% was obtained with SrCoX. The formation of active oxygen species was suppressed in the case of reaction with free radical scavengers.

#### Acknowledgments

Financial assistance and support from Department of Science and Technology and Council of Scientific and Industrial Research, India for Network programmes on Catalysis are deeply acknowledged. The authors thank Dr. P.K. Ghosh, Director, CSMCRI, for encouraging the publication of this report. They also thank the editor and reviewers for their valuable suggestions for improving the manuscript.

#### References

- [1] R.V. Grieken, J.L. Sotelo, C. Martos, J.L.G. Fierro, M.L. Granados, R. Mariscal, *Catal. Today* 61 (2000) 49.
- [2] Q. Yang, S. Wang, J. Lu, G. Xiong, Z. Feng, Q. Xin, C. Li, *Appl. Catal. A Gen.* 194–195 (2000) 507.
- [3] Q. Yang, C. Li, J.L. Wang, P. Ying, X. Xin, W. Shi, *Stud. Surf. Sci. Catal.* 130 (2000) 221.
- [4] S.B. Kumar, S.P. Mirajkar, G.C.G. Pais, P. Kumar, R. Kumar, *J. Catal.* 156 (1995) 163.
- [5] S.C. Laha, R. Kumar, *J. Catal.* 204 (2001) 64.
- [6] W. Zhang, M. Froba, J. Wang, P. Tanev, J. Wong, T.J. Pinnavaia, *J. Am. Chem. Soc.* 118 (1996) 9164.
- [7] Z. Fu, D. Yin, Q. Li, L. Zhang, Y. Zhang, *Microporous Mesoporous Mater.* 29 (1999) 351.
- [8] V.R. Choudhary, N.S. Patil, S.K. Bhargava, *Catal. Lett.* 89 (2003) 55.
- [9] N.S. Patil, R. Jha, B.S. Uphade, S.K. Bhargava, V.R. Choudhary, *Appl. Catal. A Gen.* 275 (2004) 87.
- [10] N.S. Patil, B.S. Uphade, P. Jana, S.K. Bhargava, V.R. Choudhary, *J. Catal.* 223 (2004) 236.
- [11] C.V. Rode, U.N. Nehete, M.K. Dongare, *Catal. Commun.* 4 (2003) 365.
- [12] R.A. Sheldon, J.K. Kochi, *Metal-Catalysed Oxidation of Organic Compounds*, Academic Press, New York, 1981.
- [13] J.D. Koola, J.K. Kochi, *J. Org. Chem.* 52 (1987) 4545.
- [14] A. Zombeck, D.E. Hamilton, R.S. Drago, *J. Am. Chem. Soc.* 104 (1982) 6782.
- [15] D.E. Hamilton, R.S. Drago, A. Zombeck, *J. Am. Chem. Soc.* 109 (1987) 374.
- [16] B. Rhodes, S. Rowling, P. Tidswell, S. Woodward, S.M. Brown, *J. Mol. Catal. A Chem.* 116 (1997) 375.
- [17] M.J. da Silva, P. Robles-Dutenhefner, L. Menini, E.V. Gusevskaya, *J. Mol. Catal. A Chem.* 201 (2003) 71.
- [18] G. Sankar, R. Raja, J.M. Thomas, *Catal. Lett.* 55 (1998) 15.
- [19] J.M. Thomas, R. Raja, G. Sankar, R.G. Bell, *Nature* 398 (1999) 227.
- [20] I. Belkhir, A. Germain, F. Fajula, E. Fache, *J. Chem. Soc. Faraday Trans.* 94 (1998) 1761.
- [21] A.F. Masters, J.K. Beattie, A.L. Roa, *Catal. Lett.* 75 (2001) 159.
- [22] J.M. Thomas, R. Raja, *Chem. Commun.* (2001) 675.
- [23] J.M. Thomas, *Angew. Chem. Int. Ed. Engl.* 38 (1999) 3588.
- [24] D. Dhar, Y. Kolytyn, A. Gedanken, S. Chandrasekaran, *Catal. Lett.* 86 (2003) 197.

- [25] C.L. Hill, C.M. Prosser-McCartha, *Coord. Chem. Rev.* 143 (1995) 407.
- [26] R.I. Kureshy, N.H. Khan, S.H.R. Abdi, A.K. Bhatt, P. Iyer, *J. Mol. Catal. A Chem.* 121 (1997) 25.
- [27] R. Raja, G. Sankar, J.M. Thomas, *Chem. Commun.* (1999) 829.
- [28] R. Neumann, M. Dahan, *Nature* 388 (1997) 353.
- [29] Y. Nishiyama, Y. Nakagawa, N. Mizuno, *Angew. Chem. Int. Ed. Engl.* 40 (2001) 3639.
- [30] T. Pruß, D.J. Macquarrie, J.H. Clark, *Appl. Catal. A Gen.* 276 (2004) 29.
- [31] R.M. Barrer, *Zeolites and Clay Minerals as Sorbents and Molecular Sieves*, Academic Press, London, 1978.
- [32] D.W. Breck, *Zeolite Molecular Sieves*, Wiley-Interscience, New York, 1974.
- [33] E.Y. Choi, Y. Kim, Y.W. Han, K. Seff, *Microporous Mesoporous Mater.* 41 (2000) 61.
- [34] D. Base, K. Seff, *Microporous Mesoporous Mater.* 33 (1999) 265.
- [35] Q. Tang, Y. Wang, J. Liang, P. Wang, Q. Zhang, H. Wan, *Chem. Commun.* (2004) 440;  
Q. Tang, Q. Zhang, H. Wu, Y. Wang, *J. Catal.* 230 (2005) 384;  
J. Liang, Q. Zhang, H. Wu, G. Meng, Q. Tang, Y. Wang, *Catal. Commun.* 5 (2004) 665.
- [36] J. Sebastian, R.V. Jasra, US patent application 11/375,697, March 14, 2006;  
J. Sebastian, R.V. Jasra, PCT 0549, March 14, 2006.
- [37] J. Sebastian, R.V. Jasra, *Ind. Eng. Chem. Res.* 44 (2005) 8014.
- [38] A.A. Verberckmoes, B.M. Weckhuysen, R.A. Schoonheydt, *Microporous Mesoporous Mater.* 22 (1998) 165.
- [39] G.D. Yadav, A.A. Pujari, *Org. Process Res. Dev.* 4 (2000) 88.
- [40] V.I. Iliev, A.I. Ileva, L.D. Dimitrov, *Appl. Catal.* 126 (1995) 333.
- [41] V. Rives, M.A. Ulibarri, *Coord. Chem. Rev.* 181 (1999) 61.
- [42] A.E. Martell, D.T. Sayer, *Oxygen Complexes and Oxygen Activation by Transition Metals*, Plenum Press, New York, 1988, p. 87.
- [43] T. Punniyamurthy, M.M. Reddy, S.J.S. Karla, J. Iqbal, *Pure Appl. Chem.* 68 (1996) 619.
- [44] H. Nishide, A. Suzuki, E. Tsuchida, *Bull. Chem. Soc. Jpn.* 70 (1997) 2317.
- [45] J.P. Collman, *Acc. Chem. Res.* 10 (1977) 265.
- [46] R.D. Jones, D.A. Summerville, Z.F. Basolo, *Chem. Rev.* 79 (1979) 139.
- [47] E. Tsuchida, H. Nishide, *Top. Curr. Chem.* 132 (1986) 64.
- [48] R.J. Davies, *J. Catal.* 216 (2003) 396.
- [49] X. Liu, K.-K. Iu, J.K. Thomas, *J. Phys. Chem.* 98 (1994) 7877.
- [50] X. Liu, K.-K. Iu, J.K. Thomas, *Chem. Phys. Lett.* 204 (1993) 163.
- [51] S. Hashimoto, *J. Chem. Soc. Faraday Trans.* 93 (1997) 4401.
- [52] Y.S. Park, S.Y. Um, K.B. Yoon, *J. Am. Chem. Soc.* 121 (1999) 3193.
- [53] H.J.D. McManus, C. Finel, L. Kevan, *Radiat. Phys. Chem.* 45 (1995) 761.
- [54] M. Alvaro, H. Garcia, S. Garcia, F. Marquez, J.C. Scaiano, *J. Phys. Chem. B* 101 (1997) 3043.
- [55] M. Huang, S. Kaliaguine, *J. Chem. Soc. Faraday Trans.* 88 (1992) 751.
- [56] L. Yang, Y. Aizhen, X. Qinhua, *Appl. Catal.* 67 (1991) 169.
- [57] E.J. Doskocil, S.V. Bordawekar, B.G. Kaye, R.J. Davis, *J. Phys. Chem. B* 103 (1999) 6277;  
E.J. Doskocil, S. Bordawekar, R.J. Davis, in: *Catalysis*, vol. 15, Royal Society of Chemistry, 2000, chap. 2, p. 50 and references therein.
- [58] R.T. Sanderson, *Chemical Bonds and Bond Energy*, Academic Press, New York, 1976, p. 218;  
The partial charge on oxygen atom is calculated using the following equations,  $[(\delta_{\text{q}})_{\text{O}}] = (S_{\text{E,int}} - S_{\text{E,O}}) / (\Delta S_{\text{E,O}})$ , where  $S_{\text{E,int}} = (\prod S_{\text{E,Z}}^x)^{1/\sum x}$ ,  $\Delta S_{\text{E,O}} = 2.08 (S_{\text{E,O}})^{1/2}$ ,  $S_{\text{E,O}}$  is the individual electronegativity of element Z and  $x$  is the atomic ratio of the element Z present.
- [59] R.M. Martin-Aranda, M.F. Portela, L.M. Madeira, F. Freire, M. Oliveira, *Appl. Catal. A Gen.* 127 (1995) 201.
- [60] D.D. Perrin, W.L.F. Armarego, D.R. Perrin, *Purification of Laboratory Chemicals*, second ed., Pergamon Press, Oxford, 1980.